cGAS/STING signaling in the regulation of rheumatoid synovial aggression

Ruiru Li[1#], Wei Lin[1#], Yu Kuang[1#], Jingnan Wang[1], Siqi Xu[1], Chuyu Shen[1], Qian Qiu[1], Maohua Shi[2], Youjun Xiao[1], Liuqin Liang[1], Hanshi Xu[1]

[1]Department of Rheumatology and Immunology, the First Affiliated Hospital, Sun Yat-sen University, Guangzhou, China; [2]Department of Rheumatology, the First People's Hospital of Foshan, Foshan, China

Contributions: (I) Conception and design: R Li, W Lin, Y Kuang, J Wang, S Xu; (II) Administrative support: L Liang, Y Xiao, H Xu; (III) Provision of study materials or patients: M Shi, Y Kuang, L Liang; (IV) Collection and assembly of data: C Shen, Q Qiu, Y Xiao; (V) Data analysis and interpretation: R Li, W Lin, Y Kuang, Y Xiao, H Xu; (VI) Manuscript writing: All authors; (VII) Final approval of manuscript: All authors.

[#]These authors contributed equally to this work.

Correspondence to: Hanshi Xu; Liuqin Liang; Youjun Xiao. Department of Rheumatology and Immunology, the First Affiliated Hospital, Sun Yat-sen University, Guangzhou, Guangdong, China. Email: xuhanshi@mail.sysu.edu.cn; lliuq@mail.sysu.edu.cn; xiaoyouj@mail2.sysu.edu.cn.

Background: Fibroblast-like synoviocytes (FLSs) play a critical role in promoting synovial aggression and joint destruction in rheumatoid arthritis (RA). Cyclic GMP-AMP synthase (*cGAS*)/stimulator of interferon gene (*STING*) signaling plays an important role in controlling a series of cellular biological processes. However, it is still unclear whether *cGAS/STING* signaling regulates rheumatoid synovial aggression.

Methods: Cell migration and invasion were detected using a Transwell chamber. Gene expression was measured using quantitative reverse transcription-polymerase chain reaction (qRT-PCR), and protein expression was detected by western blotting. Reactive oxygen species (ROS) levels were measured by 2',7'-di chlorodihydrofluorescein diacetate (DCFH-DA) probe. F-actin staining and immunofluorescence assays were used to investigate lamellipodia formation and nuclear translocation, respectively. A severe combined immunodeficiency (SCID) mouse model was established to observe the migration and invasion of RA FLSs *in vivo*.

Results: Our results showed that cytosolic double-stranded DNA (dsDNA)-induced *cGAS/STING* activation promoted the *in vitro* migration and invasion of RA FLSs. Moreover, RA FLSs treated with *cGAS* or *STING* short hairpin RNA (shRNA) exhibited reduced invasion into cartilage in the SCID model. Mechanistically, we determined that *cGAS/STING* activation leads to increased mitochondrial ROS levels, and thereby increases phosphorylation of mammalian sterile 20-like kinase 1 (*MST1*), a core component of the Hippo pathway, subsequently promoting activation of forkhead box1 (*FOXO1*). *MST1* and *FOXO1* knockdown also diminished the migration and invasion of RA FLSs.

Conclusions: Our findings suggest that *cGAS/STING* signaling has an important role in regulating rheumatoid synovial aggression and that targeting *cGAS/STING* may represent a novel potential therapy for RA.

Keywords: Cyclic GMP-AMP synthase/stimulator of interferon gene (*cGAS/STING*); mammalian sterile 20-like kinase 1 (*MST1*); rheumatoid arthritis (RA); fibroblast-like synoviocytes (FLSs); invasion

Submitted Aug 29, 2021. Accepted for publication Dec 19, 2021.
doi: 10.21037/atm-21-4533
View this article at: https://dx.doi.org/10.21037/atm-21-4533

Introduction

Rheumatoid arthritis (RA) is a common autoimmune disorder characterized by persistent inflammation and joint destruction. Fibroblast-like synoviocytes (FLSs), which exhibit "tumorlike" properties, including increased migration and invasion, hyperproliferation, and apoptosis resistance, have a critical role in controlling synovial aggression and joint destruction (1). An increasing amount of evidence indicates that targeting FLSs might be a novel strategy for controlling joint damage in RA (2,3). However, the precise underlying mechanisms for regulating the development of the invasive phenotype of RA FLSs are still undefined.

Cytosolic DNA is a powerful activator of the innate immune system and figures prominently in autoimmune diseases. Cytosolic DNA is derived from multiple sources, including viral and bacterial pathogens or self-DNA, such as damaged mitochondrial DNA, leaked/damaged nuclear DNA, and cytosolic DNA in micronuclei (4). A previous study found elevated double-stranded DNA (dsDNA) levels in the synovial fluid of patients with RA. Interestingly, dsDNA from RA synovial fluid can induce joint inflammation *in vivo* (5). Our previous study also demonstrated that the accumulation of cytosolic dsDNA in RA FLSs contributes to the inflammatory response (6). Cyclic guanosine monophosphate-adenosine monophosphate (GMP-AMP) synthase (*cGAS*), which serves as a key cytosolic DNA sensor, activates the stimulator of interferon genes (*STING*), thereby promoting type I interferon (*IFN*) production and causing an inflammatory response in turn (4). Our previous study showed that the accumulation of cytosolic dsDNA induces *cGAS/STING* activation, which promotes the proinflammatory cytokine secretion in RA FLSs, suggesting an important role for cytosolic dsDNA-mediated *cGAS/STING* activation in rheumatoid synovial inflammation (6). Interestingly, recent studies have indicated that *cGAS/STING* pathway activation is involved in modulating migration, invasion, and proliferation in some cell lines (7,8). However, it is unknown whether the *cGAS/STING* signaling pathway plays a role in regulating rheumatoid synovial aggression and joint destruction.

Protein kinase mammalian sterile 20-like kinase 1 (*MST1*), as the core component of the Hippo signaling pathway, has been implicated in the downstream control of the *cGAS/STING* pathway in endothelial cell migration and angiogenesis process (8). Previous studies have suggested the importance of *MST1/2* in regulating cytoskeleton remodeling and integrin activation in lymphocytes (9). We were thus interested in exploring whether *MST1* mediates the role of *cGAS/STING* signaling in modulating migration and the cytoskeleton in RA FLSs. We present the following article in accordance with the MDAR (Materials Design Analysis Reporting) reporting checklist (available at https://atm.amegroups.com/article/view/10.21037/atm-21-4533/rc).

Methods

Materials

dsDNA (ISD) and polymerase chain reaction (PCR) primers were synthesized by Sangon Company (Shanghai, China; sequences listed in Table S1). Primary antibodies against *cGAS* (rabbit), *STING* (rabbit), *p-MST1* (Thr183, rabbit), *MST1* (rabbit), forkhead box1 (*FOXO1*, rabbit), and β-actin (mouse) were purchased from Cell Signaling Technology (Danvers, MA, USA). *p-FOXO1* (Ser212, rabbit) was purchased from Invitrogen (Waltham, MA, USA).

Preparation of human FLSs

Twenty active patients with RA from the First Affiliated Hospital, Sun Yat-sen University who were undergoing joint replacement or synovectomy were enrolled in our study. RA was diagnosed according to classification criteria of the 2010 American College of Rheumatology/European League Against Rheumatism (ACR/EULAR) (10). The study was conducted in accordance with the Declaration of Helsinki (as revised in 2013). This study was approved by the Medical Ethics Committee of the First Affiliated Hospital, Sun Yat-sen University, China (No. [2017]049). All patients provided informed consent before participating in the study. The backgrounds of the RA patients are summarized in Table S2.

To isolate FLSs, synovial tissues were cut into small pieces and digested with collagenase for 2 hours at 37 ℃. Isolated FLSs were grown in Dulbecco's Modified Eagle Medium/F-12 (DMEM/F12) containing 10% fetal bovine serum (FBS), 100 U/mL penicillin, and 100 μg/mL streptomycin. At confluence, FLSs were routinely trypsinized, passaged, and used from passages 4 to 6.

For lentiviral transduction, cells were inoculated with lentivirus (GeneChem, Shanghai, China) at subconfluence in the presence of 10 μg/mL polybrene. After transfection

for 8 hours, the media were replaced with fresh media. The target sequences of short hairpin RNA (shRNAs) are listed in Table S3.

Real-time PCR

Total RNA was extracted from FLSs and reverse-transcribed by using PrimeScript RT Master Mix (Takara, Shiga, Japan) according to the manufacturer's protocol. Quantitative reverse transcription-polymerase chain reaction (qRT-PCR) analysis was performed using a Light Cycler 480 Real-Time PCR Detection System (Roche, Basel, Switzerland) and SYBR Premix Ex Taq (Takara) according to the manufacturers' instructions. The relative messenger RNA (mRNA) expression levels were normalized to the *GAPDH* (ΔCt = Ct target – Ct *GAPDH*) and compared with a calibrator using the ΔΔCt method (ΔΔCt = ΔCt sample – ΔCt calibrator). Table S1 shows the primer sequences. All experiments were performed at least 3 times.

Gene silencing

cGAS small interfering RNA (siRNA), *STING* siRNA, *MST1* siRNA, *FOXO1* siRNA, and yes-associated protein (*YAP*) siRNA were purchased from Ribobio (Guangzhou, China). The target sequences of the siRNAs are listed in Table S4. RA FLSs that reached 60–70% confluence were transfected with a mixture of 100 nM siRNA and 10 mg/mL Lipofectamine 3000 (Thermo Fisher Scientific, Waltham, MA, USA) for 6 hours, according to the manufacturer's protocols. Experiments were performed 48 hours after transfection. At the end of the culture, the transfection efficiency was confirmed using western blot and qRT-PCR.

In vitro migration and invasion assay of FLS

Cell migration ability was assessed with the Boyden chamber method using a filter with an 8.0-μm pore size and a 6.5 mm diameter (Corning Life Sciences, Tewksbury MA, USA). FLSs (6×10^4 cells/mL) were suspended in serum-free DMEM in the upper wells, while DMEM containing 10% FBS as a chemoattractant was placed in the lower wells. The chamber was incubated at 37 ℃ for 6 hours. After incubation, the remaining cells on the upper surface of the filter were scraped using a cotton bud. The migrated cells in the filter were fixed in methanol for 15 minutes, stained with 0.1% crystal violet for 15 minutes, and counted using an optical microscope. The stained cells were quantified as the mean number of cells per 10 random fields for each assay. Transwell chambers precoated with Matrigel matrix (BD Biosciences, Franklin Lakes, NJ, USA) were used for invasion assay.

F-actin staining

RA FLSs were cultured on 18 mm coverslips. The cells were fixed in 4% paraformaldehyde for 15 minutes and permeabilized by 0.1% Triton X-100 in phosphate-buffered saline (PBS) for 5 minutes at room temperature and then blocked in a blocking buffer for 1 hour. Cells were incubated overnight with phalloidin at 4 ℃ to detect F-actin and then stained using 4',6-diamidino-2-phenylindole (DAPI; BBI, Shanghai, China) to detect nuclei. The coverslips were mounted using fluoroshield histology mounting medium (Sigma-Aldrich, St. Louis, MO, USA) and examined using a fluorescence microscope (DMI8, Leica, Wetzlar, Germany).

Immunofluorescence

FLSs were briefly washed in PBS, fixed in 4% paraformaldehyde in PBS for 15 minutes, permeabilized with 0.1% Triton X-100 in PBS for 15 minutes, and blocked in a blocking buffer for 1 hour at room temperature. After incubation with diluted primary antibodies overnight at 4 ℃ and fluorochrome-conjugated secondary antibody (Invitrogen) for 1 hour at room temperature, the cell nuclei were stained using DAPI (BBI) and imaged using fluoroshield histology mounting medium (Sigma-Aldrich).

Western blotting

Protein concentrations were quantified using the bicinchoninic acid (BCA) protein assay (Thermo Fisher Scientific). The cell lysates prepared in sodium dodecyl sulfate- polyacrylamide gel electrophoresis (SDS-PAGE) Sample Loading Buffer (Beyotime, Shanghai, China) were separated by 10–12% SDS-PAGE and transferred onto a 0.2-μm polyvinylidene fluoride (PVDF) membrane (Millipore, Burlington, MA, USA). The PVDF membranes were incubated with indicated primary antibodies diluted 1:1,000 for *cGAS*, *STING*, *p-MST1*, *MST1*, *p-FOXO1*, *FOXO1*, *LATS1*, and *YAP*.

Intracellular ROS detection

2',7'-dichlorodihydrofluorescein diacetate (DCFH-DA)

(Beyotime) was used to detect intracellular ROS levels of FLSs. FLSs were incubated with 10 μM of DCFH-DA in serum-free DMEM/F12 at 37 ℃ for 20 minutes. Cells were washed 3 times to remove excessive DCFH-DA and subjected to flow cytometry (CytoFLEX S, Beckman Coulter, Brea, CA, USA), with an emission wavelength of 525 nm and an excitation wavelength of 488 nm.

Assessment of the in vivo invasion of RA FLSs into human cartilage implants

RA FLSs (4×10^5) were suspended in 100 μL of sterile saline and absorbed by a gelatin sponge (80 mm^3). Human cartilage obtained from non-arthritic trauma patients undergoing knee surgery was cut into pieces and inserted into the sponge. For implantation, each sponge containing cartilage and RA FLSs was placed under the skin on the left flanks of 4-week-old SCID mice (Sun Yat-sen University Laboratory Animal Center, Guangzhou, China). All mice were housed under specific pathogen-free (SPF) conditions and allowed free access to water and food. After 50 days of implantation, the implants were taken out from the mice, and the mice were killed. Each explant specimen was stained with hematoxylin and eosin (HE). FLS invasion into cartilage was graded as previously described (11). The invasiveness level was scored as follows: 0 = no or minimal invasion, 1 = visible invasion (2-cell depth), 2 = invasion (5-cell depth), and 3 = deep invasion (more than 10-cell depth). Each specimen was evaluated in a blinded manner by 2 experienced investigators. All procedures involving animals were approved by the Institutional Animal Care and Use Committee (IACUC) of Sun Yat-sen University (No. SYSU-IACUC-2021-000028) and conducted according to the guidelines of the Chinese Ethics Committee for the care and use of animal research.

Statistical analysis

All statistical analyses of the data were performed using SPSS 13.0 (IBM Corp., Armonk, NY, USA) and analyzed in a blinded manner. Data are expressed as the means ± standard error of the mean (SEM). Presented values were derived from at least 3 independent experiments. A 2-tailed Student's *t*-test was used to analyze the differences between 2 groups, and 1-way analysis of variance (ANOVA) analysis of variance with Bonferroni's post hoc comparisons was used to analyze 3 or more groups in normally distributed data. We used nonparametric tests (Mann-Whitney rank-sum test for 2 groups or the Kruskal-Wallis 1-way analysis among 3 groups for continuous variables) to compare the differences between different groups in abnormal distribution data. P values less than 0.05 were considered significant.

Results

The cGAS/STING pathway regulated cytosolic dsDNA-induced migration and invasion of RA FLSs

The abnormal migration and invasion of FLSs play a key role in controlling rheumatoid synovial aggression and joint destruction. Our previous study found an increased accumulation of cytosolic dsDNA and expression of *cGAS* and *STING* in FLSs and synovial tissues from patients with RA. In addition, a positive correlation between the *cGAS* immunoreactive score (IRS) and synovitis score was observed (6). Herein, we evaluated the role of cytosolic dsDNA-mediated *cGAS/STING* signaling in regulating the migration and invasion of RA FLSs. Specific siRNAs were used to inhibit *cGAS* or *STING* expression. As shown in *Figure 1A*, transfection with all 3 siRNA oligonucleotides decreased *cGAS* or *STING* expression; however, the inhibitory effect of siRNA-1 and siRNA-2 on *cGAS* or siRNA-2 and siRNA-3 on *STING* was more prominent. Thus, siRNA-1 and siRNA-2 for *cGAS* or siRNA-2 and siRNA-3 for *STING* were used for further experiments. We transfected ISD dsDNA (45 bp dsDNA) into the RA FLSs to activate the *cGAS/STING* pathway. As shown in *Figure 1B*, treatment with ISD dsDNA promoted the migration of RA FLSs; however, this promotion was mitigated in *cGAS* or *STING* siRNA-transfected RA FLSs. Since the ability to invade cartilage and bone is a critical pathogenic behavior of RA FLSs, we examined the effect of *cGAS* or *STING* suppression on modulating the invasive behavior of RA FLSs using Matrigel-coated Transwell membranes. We determined that ISD dsDNA stimulation increased the invasion of RA FLSs, whereas the transfection with *cGAS* or *STING* siRNA diminished ISD dsDNA-induced invasion of RA FLSs (*Figure 1C*).

Cell migration requires the dynamic reorganization of the actin cytoskeleton. We used fluorescent phalloidin staining to observe polymerized actin in ISD-induced migrating cells after wounding in *cGAS*- or *STING*-inhibited RA FLSs. As shown in *Figure 1D*, RA FLSs with ISD stimulation displayed lamellipodia, while RA FLSs with *cGAS* or *STING* knockdown exhibited reduced formation of lamellipodia. Our data indicate a role for the *cGAS/STING*

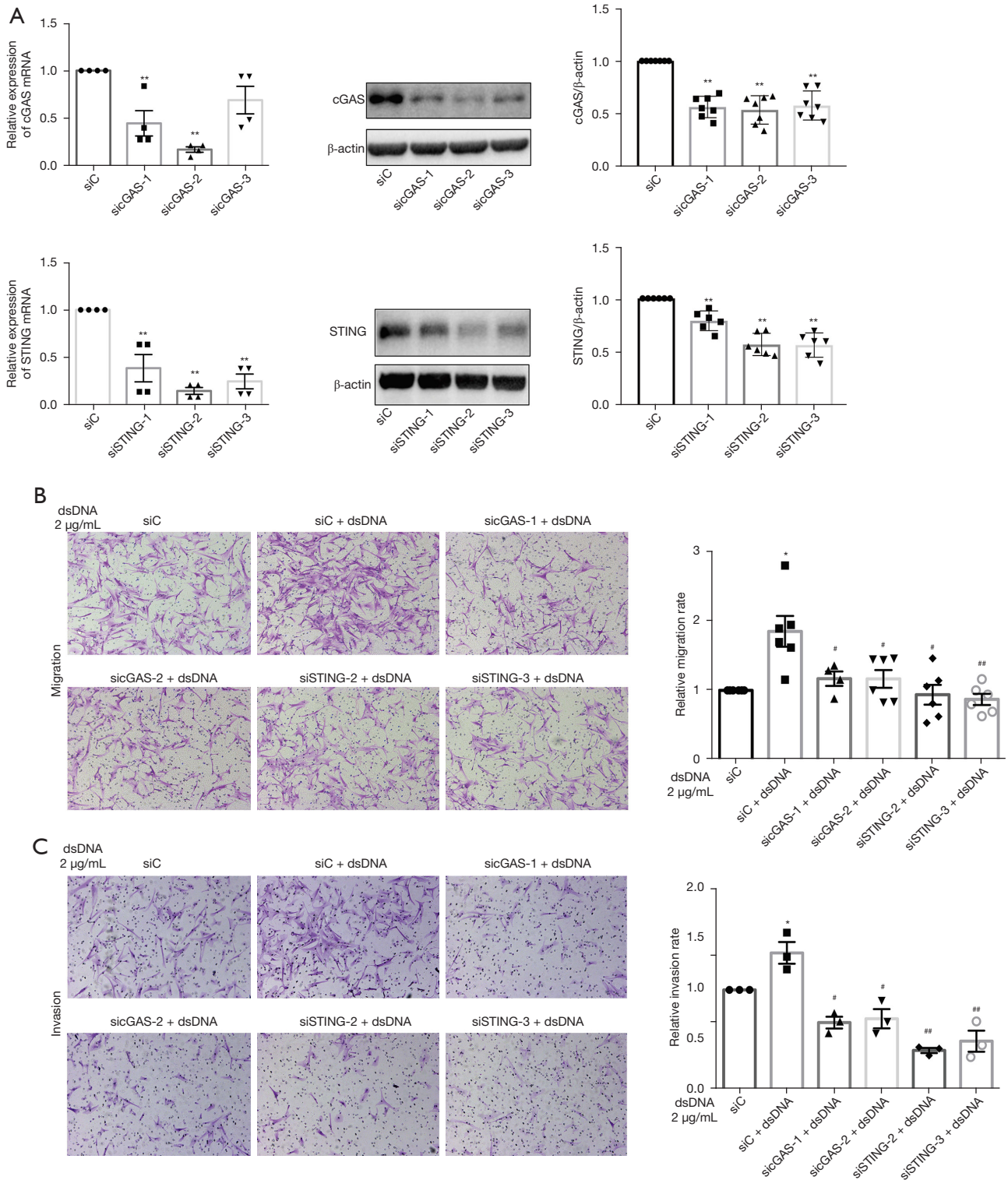

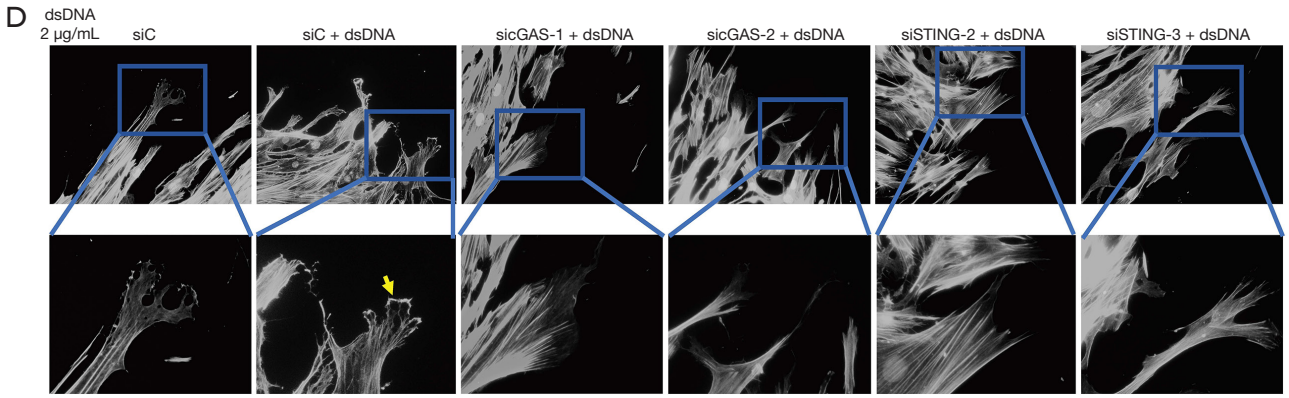

Figure 1 Effects of *cGAS/STING* knockdown on the migration and invasion of RA FLSs induced by cytosolic dsDNA. RA FLSs were transfected with siRNA or ISD dsDNA (2 μg/mL). (A) RA FLSs were transfected with *cGAS* or *STING* siRNA (*sicGAS*1-3 or *siSTING*1-3) or control siRNA (siC) for 48 hours and subjected to qRT-PCR analysis for mRNA expression or western blot analysis for protein expression. A representative blot of at least 3 independent experiments is shown. (B,C) Migration and invasion of RA FLSs were measured using a Transwell assay. Invasion was evaluated using inserts coated with matrigel basement membrane matrix. The relative migratory or invasive rate was calculated by counting migrated or invaded cells and then normalized to the siC or siC + dsDNA. Migrated and invaded cells on the membrane were stained with 0.3% crystal violet. Representative images (original magnification: 100×) are shown. The graphs show the relative migration rates. (D) *cGAS* or *STING* knockdown impaired the lamellipodia formation in RA FLSs. RA FLSs were wounded and stimulated with dsDNA (2 μg/mL) for 8 hours. Representative images are shown (original magnification: 400×). The yellow arrow indicates lamellipodia formation. The data (A-C) are shown as the mean ± SEM from at least 3 independent experiments. *P<0.05; **P<0.01 *vs.* siC; $^{\#}$P<0.05; $^{\#\#}$P<0.01 *vs.* siC + dsDNA. RA, rheumatoid arthritis; FLSs, fibroblast like-synoviocytes; *cGAS*, cyclic GMP-AMP synthase; *STING*, stimulator of interferon genes; *sicGAS*, *cGAS* siRNA; *siSTING*, *STING* siRNA; siC, control siRNA; dsDNA, double-stranded DNA; qRT-PCR, quantitative reverse transcription-polymerase chain reaction.

pathway in the formation of membrane protrusions in migrating cells.

Finally, we evaluated the effect of *cGAS* or *STING* knockdown on the *in vivo* invasion of RA FLSs into cartilage using the SCID mouse coimplantation model. Specific shRNAs were used to inhibit *cGAS* or *STING* expression. As shown in *Figure 2A*, transfection with all 3 lentiviral shRNAs decreased *cGAS* or *STING* expression; however, the inhibitory effect of shRNA-1 and shRNA-3 on *cGAS* or shRNA-2 and shRNA-3 on *STING* was more prominent. Thus, shRNA-1 and shRNA-3 for *cGAS* or shRNA-2 and shRNA-3 for *STING* were used for subsequent experiments. RA FLSs carrying *cGAS* or STING shRNA or empty vector were coimplanted side by side into the left or right flanks of SCID mice. RA FLSs transfected with *cGAS* or *STING* shRNA exhibited a significantly decreased of invasion into cartilage as compared to the cells transfected with empty vector (*Figure 2B*). Collectively, our findings suggested that the *cGAS/STING* pathway is important for regulating the migration and invasion of RA FLSs.

MST1 mediated the cGAS/STING regulation of RA FLS function

A previous study showed that the *cGAS/STING* pathway is involved in cell migration through regulating the activation of *MST1* (8). Therefore, we investigated whether *MST1* mediates the role of the *cGAS/STING* pathway in the cytosolic dsDNA-induced migration and invasion of RA FLSs. As shown in *Figure 3A*, ISD dsDNA transfection promoted *MST1* phosphorylation with a peak at 2 hours; however, this promotion was mitigated by *cGAS* or *STING* knockdown (*Figure 3B*).

We further determined the role of *MST1* in RA FLS migration and invasion by using 2 specific *MST1* siRNAs to inhibit *MST1* expression (*Figure 3C*). We found that *MST1* knockdown inhibited the enhanced ISD dsDNA-induced migration and invasion of RA FLSs (*Figure 3D*). Consistent with our findings regarding migration and invasion, RA FLSs with *MST1* knockdown exhibited decreased formation of lamellipodia (*Figure 3E*). These data suggested that *MST1* acts downstream of the *cGAS/STING* pathway in the

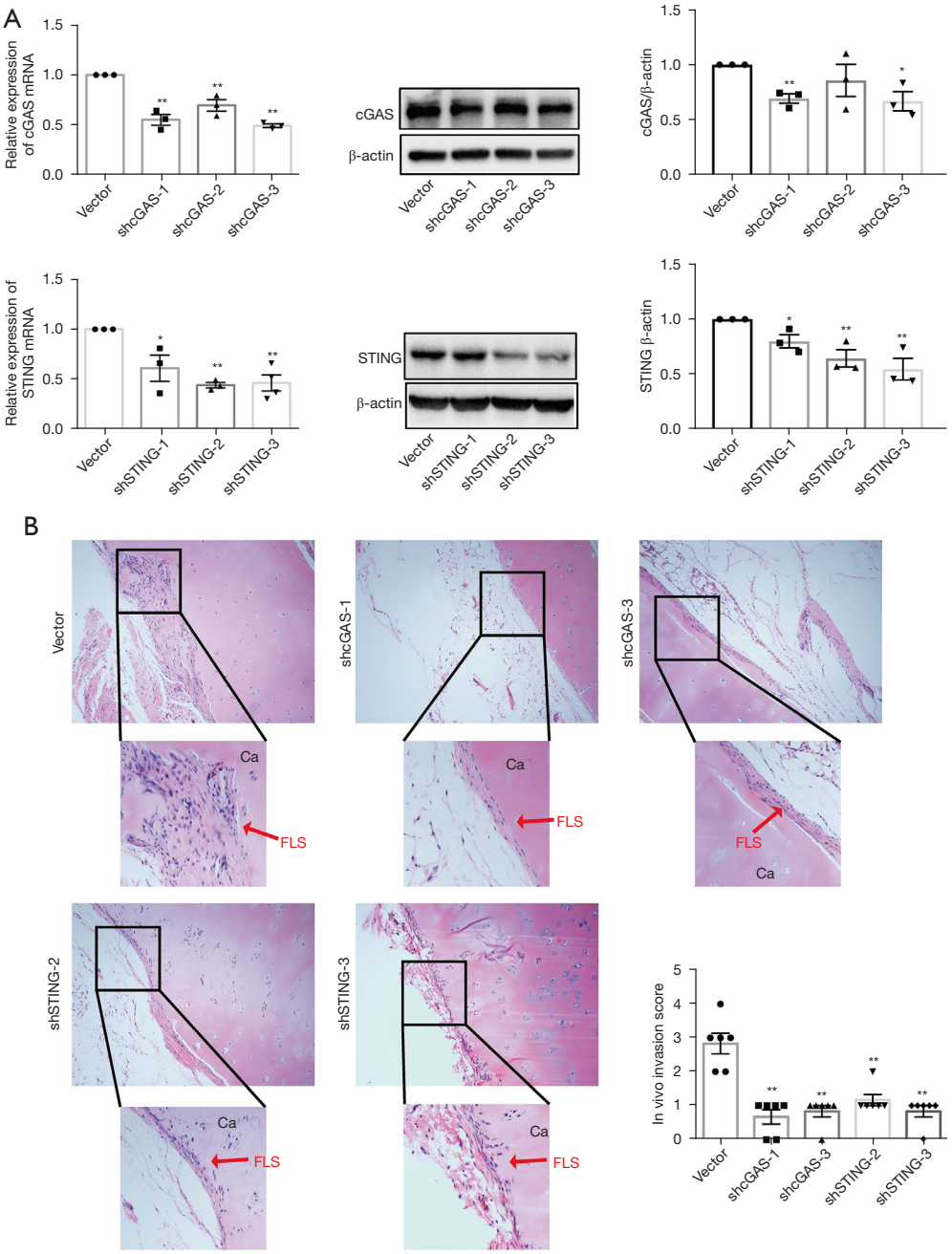

Figure 2 The effect of *cGAS* or *STING* inhibition on the invasion of RA FLSs into human cartilage implants transferred under the skin of SCID mice. (A) RA FLSs were transfected with *cGAS* or *STING* shRNA (*shcGAS*1-3 or *shSTING*1-3) or control vectors for 48 hours and subjected to qRT-PCR analysis for mRNA expression or western blot analysis for protein expression. A representative blot of 3 independent experiments is shown. (B) RA FLSs, transfected with vector, *cGAS* or *STING* shRNA were transferred side by side into the left or right flanks of the SCID mouse model (n=6 for each group). The mice were killed after 50 days, and implants were stained with haematoxylin and histologically evaluated for cell invasion. The arrows indicate RA FLSs invading Ca (upper image; original magnification: 200×). Data represent the mean mean ± SEM of semiquantitative analysis. *P<0.05; **P<0.01 *vs.* vector. RA, rheumatoid arthritis; FLSs, fibroblast like-synoviocytes; *cGAS*, cyclic GMP-AMP synthase; *STING*, stimulator of interferon genes; *sicGAS*, *cGAS* siRNA; *siSTING*, *STING* siRNA; siC, control siRNA; dsDNA, double-stranded DNA; Ca, cartilage; SCID, severe combined immunodeficiency; qRT-PCR, quantitative reverse transcription-polymerase chain reaction.

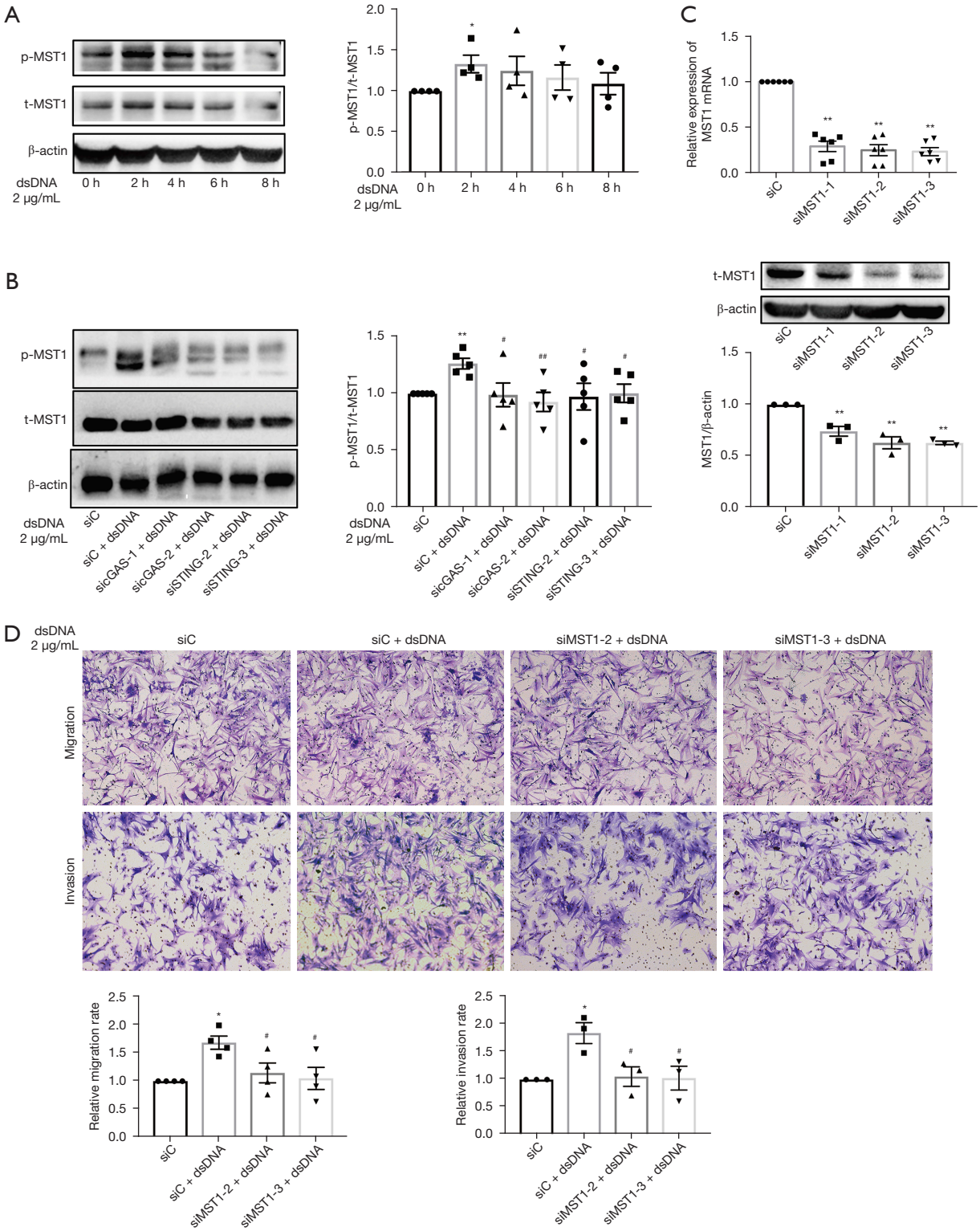

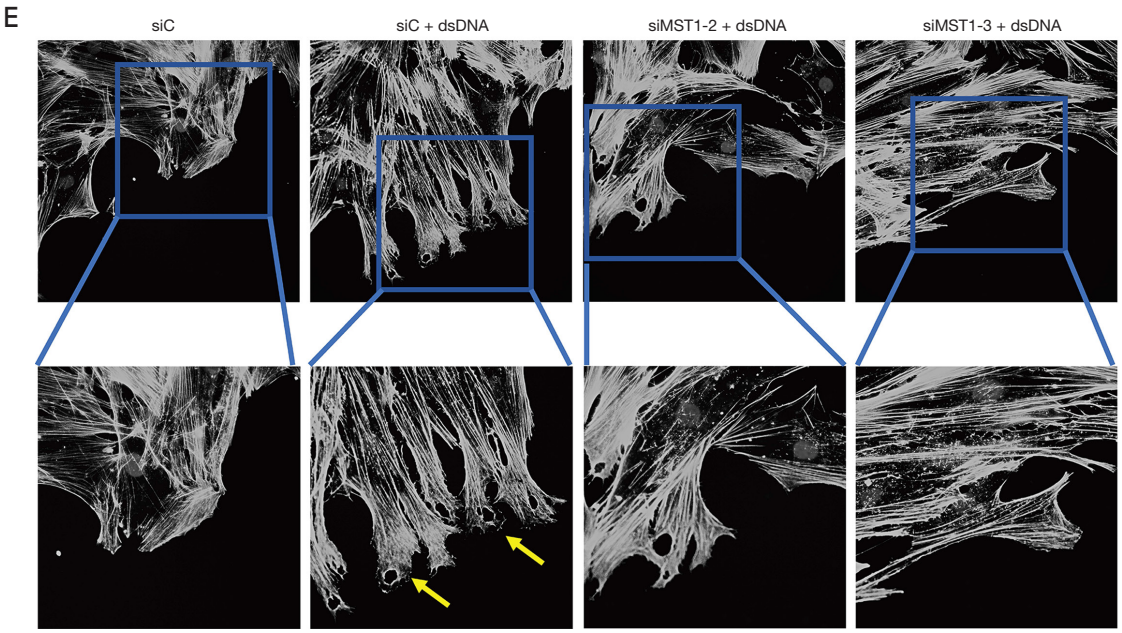

Figure 3 The effect of *cGAS/STING* inhibition on *MST1* activation. (A) The effect of ISD dsDNA transfection on *MST1* phosphorylation. RA FLSs were transfected with ISD dsDNA (2 μg/mL) for different times (2, 4, 6, and 8 hours). Western blotting was used to detect the expression of total and phosphorylated *MST1*. (B) RA FLSs, transfected with *cGAS* or *STING* siRNA, or control siRNA, were serum-starved overnight and then transfected with dsDNA (2 μg/mL) for 2 hours. Representative images of immunoblots (left panel) and densitometric quantification (right panel) of phosphorylated *MST1* expression are shown. (C) Efficiency of MST1 knockdown. RA FLSs were transfected with *MST1* siRNA (*siMST1*-1-3) or siC for 48 hours and subjected to qRT-PCR analysis and western blot analysis. (D) The effect of *MST1* knockdown on migration and invasion. RA FLSs, transfected with *MST1* siRNA, were serum-starved overnight and then transfected with ISD dsDNA (2 μg/mL) for 8 hours. Migration and invasion were measured using a Boyden chamber. The relative migration and invasion rate was calculated by counting migrated or invaded cells and was followed by normalization to the siC. Migrated and invaded cells on the membrane were stained with 0.3% crystal violet. Representative images (original magnification: 100×) are shown. Graphs show the relative migratory and invasive rates. (E) The effect of *MST1* knockdown on lamellipodia formation of RA FLSs. Representative images are shown (original magnification: 400×). The yellow arrows indicate lamellipodia formation. A representative blot of at least 3 independent experiments is shown. The data (A-D) are shown as the mean ± SEM from at least 3 independent experiments. *P<0.05; **P<0.01 *vs.* siC; $^{\#}$P<0.05; $^{\#\#}$P<0.01 *vs.* siC + dsDNA. *MST1*, mammalian sterile 20-like kinase 1; RA, rheumatoid arthritis; FLSs, fibroblast like-synoviocytes; *cGAS*, cyclic GMP-AMP synthase; *STING*, stimulator of interferon genes; *sicGAS*, cGAS siRNA; *siSTING*, *STING* siRNA; siC, control siRNA; dsDNA, double-stranded DNA; *siMST1*, *MST1* siRNA; qRT-PCR, quantitative reverse transcription-polymerase chain reaction.

cytosolic dsDNA-induced migration and invasion of RA FLSs.

MST1 regulated the migration and invasion of RA FLSs independent of the canonical Hippo pathway

To determine whether canonical large tumor suppressor kinase 1 (*LATS1*) and *YAP* are the downstream regulators of *MST1* in RA FLSs, we assessed the effect of *MST1* inhibition on *LATS1* and *YAP* protein expression. We discovered that *MST1* knockdown did not influence the protein expression of *LATS1* or *YAP* (*Figure 4*). These findings suggested that *MST1* does not use the canonical Hippo signaling pathway for directing migration of RA FLSs.

FOXO1 mediated MST1 regulation for the migration and invasion of RA FLSs

In canonical signaling, *MST1/2* activation leads to phosphorylation of *LATS1/2*, and subsequently regulates the Hippo pathway effector Yorkie (*YAP*/TAZ) (12). Thus,

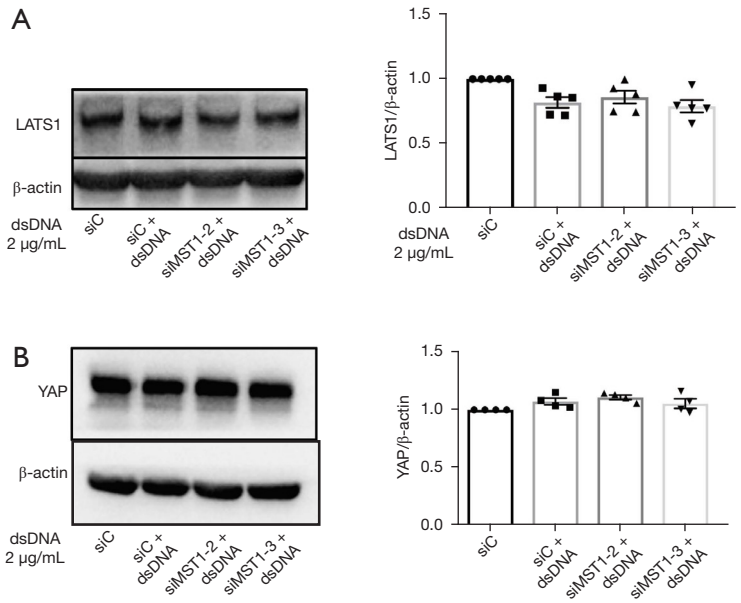

Figure 4 The effects of *MST1* knockdown on canonical *LATS1* and *YAP* protein expression in RA FLSs. RA FLSs, transfected with *cGAS* or *STING* siRNA or control siRNA, were serum-starved overnight and transfected with dsDNA (2 μg/mL) for 8 hours. (A) *LATS1* and (B) *YAP* protein expression was measured using western blotting. Densitometric quantification of protein levels (right panel) is shown as the mean ± SEM from at least 3 independent experiments. *LATS1*, large tumor suppressor kinase 1; *YAP*, yes-associated protein; RA, rheumatoid arthritis; FLSs, fibroblast like-synoviocytes; *MST1*, mammalian sterile 20-like kinase 1; *siMST1*, MST1 siRNA; dsDNA, double-stranded DNA.

to explore the underlying mechanisms by which *MST1* modulates the migration and invasion of RA FLSs, we clarified the effect of *MST1* knockdown on the expression of *LATS1* and *YAP*. *MST1* knockdown did not influence the protein expression of *LATS1* or *YAP* (*Figure 4*), suggesting that *MST1* does not use the canonical Hippo pathway for the migration of RA FLSs.

Therefore, we focused on the alternative downstream effector of *MST1* beyond the canonical Hippo pathway. According to the findings on other cell types in previous reports, *FOXO1* may be a downstream cellular substrate of *MST1*. As shown in *Figure 5A*, phosphorylation of *FOXO1* reached a peak at 8 hours in response to ISD stimulation. Transfection with *MST1* siRNA decreased the phosphorylation of *FOXO1* (*Figure 5B*). Moreover, we observed that ISD dsDNA stimulation resulted in the nuclear translocation of *FOXO1* in RA FLSs; however, this translocation was reversed in *MST1* siRNAs-transfected cells (*Figure 5C*). To clarify the role of *FOXO1* in RA FLS migration and invasion, we used siRNA to knockdown *FOXO1* (*Figure 5D*). *FOXO1* siRNA-transfected RA FLSs exhibited reduced migration and invasion (*Figure 5E*). Our findings implied that FOXO1 may be a downstream substrate of MST1 for regulating the cytosolic dsDNA-induced migration and invasion of RA FLSs.

cGAS/STING regulated the level of reactive oxygen species production in RA FLSs

We next sought to gain mechanistic insights into how *cGAS/STING* modulates *MST1* expression in RA FLSs. It has been reported that *MST1* is sensitive to oxidative stress (13); therefore, we investigated whether reactive oxygen species (ROS) production is involved in the role of *cGAS/STING* in controlling *MST1*. 2',7'-dichlorodihydrofluorescein diacetate (DCFH-DA) was used to measure the ROS production. We first evaluated the effect of ISD dsDNA stimulation on ROS production and found that the ROS levels peaked 8 hours after ISD dsDNA stimulation (*Figure 6A*). The major sources of ROS include the NADPH oxidases, xanthine oxidase, and mitochondria; therefore, we used a series of pharmacological inhibitors to determine the sources of ROS induced by ISD dsDNA. Our results showed that rotenone (mitochondrial complex I inhibitor)

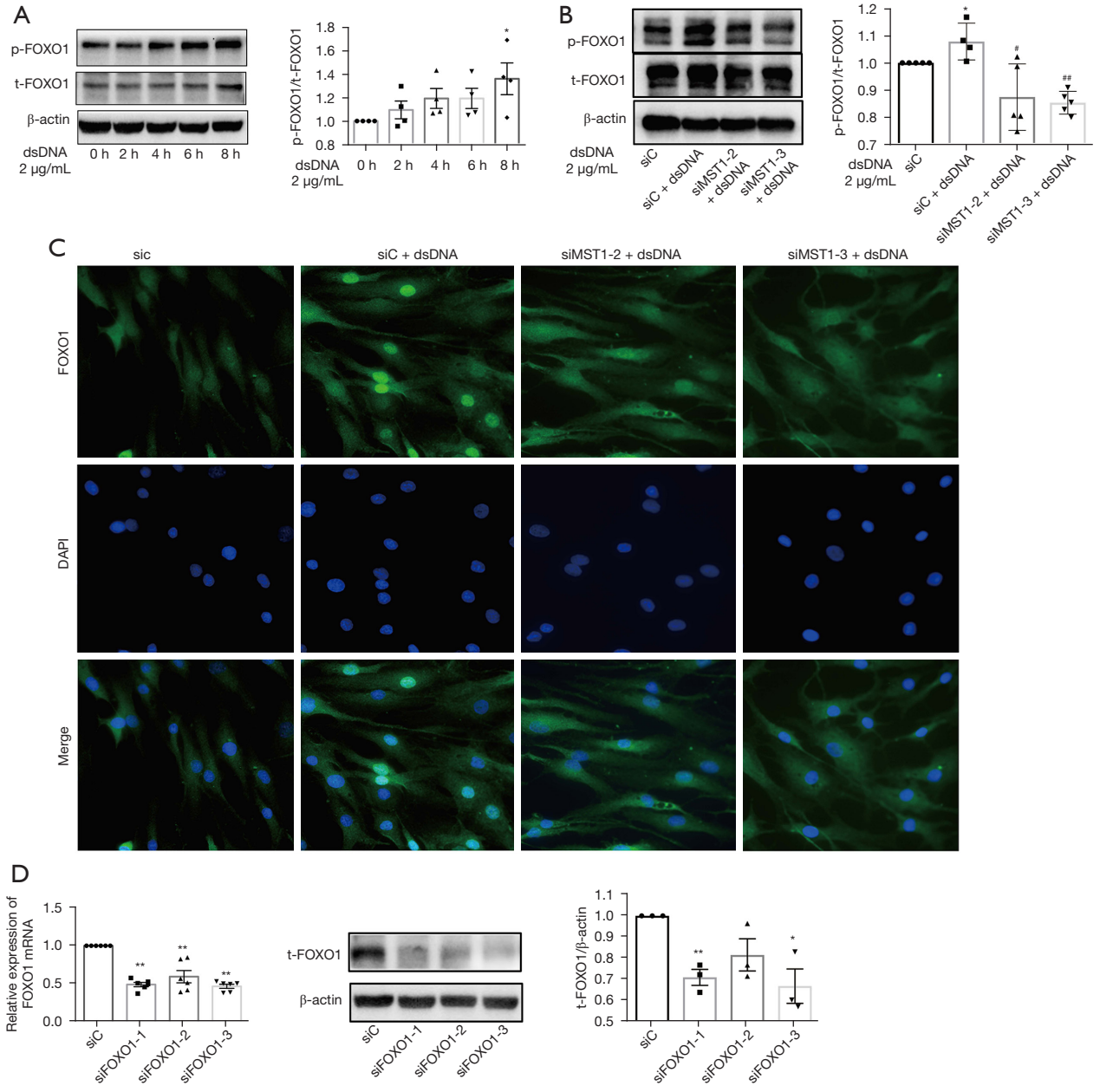

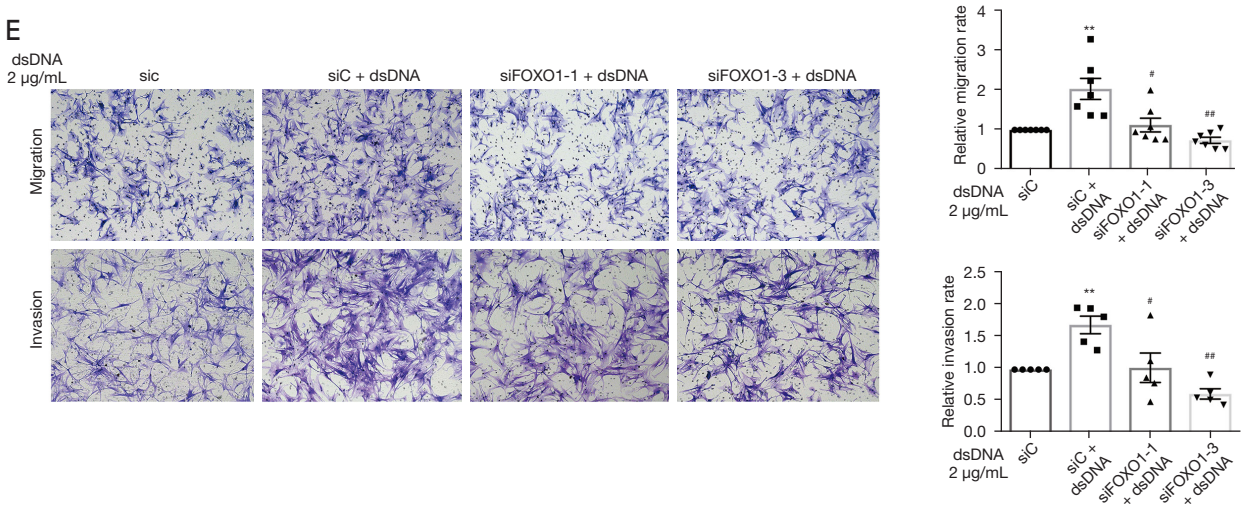

Figure 5 The effect of *MST1* knockdown on *FOXO1* activation. (A) The effect of ISD dsDNA treatment on *FOXO1* phosphorylation. RA FLSs were transfected with ISD dsDNA (2 μg/mL) for different times (2, 4, 6, and 8 hours). Protein expression was detected by western blot. (B) The effect of *MST1* knockdown on *FOXO1* phosphorylation. RA FLSs transfected with *MST1* siRNA or control siRNA were serum-starved overnight and transfected with dsDNA (2 μg/mL) for 8 hours. The *pFOXO1* and *tFOXO1* protein expression was measured using western blotting. (C) The effect of MST1 knockdown on the nuclear translocation of *FOXO1*. The translocation of *FOXO1* into the nucleus was evaluated using immunofluorescence staining. Representative immunofluorescent images of *FOXO1* (green) and nuclei (blue) in FLSs are shown. Original magnification 400×. (D) Efficiency of *FOXO1* knockdown. RA FLSs were transfected with FOXO1 siRNA (si*FOXO1*-1-3) or siC for 48 hours. The *FOXO1* mRNA and protein expression were detected by qRT-PCR and western blotting, respectively. The effect of *FOXO1* knockdown on the migration and invasion of RA FLSs. (E) RA FLSs transfected with *FOXO1* siRNA were serum-starved overnight and then transfected with ISD dsDNA (2 μg/mL) for 8 hours before migration and invasion. The relative migratory and invasive rate was calculated by counting migrated or invaded cells and through normalization to the siC or siC + dsDNA. Migrated and invaded cells on the membrane were stained with 0.3% crystal violet. Representative images (original magnification: 100×) are shown. Graphs show the relative migration rates. The data (A,B,D,E) are shown as the mean ± SEM from at least 3 independent experiments. *P<0.05; **P<0.01 *vs.* siC; $^{\#}$P<0.05; $^{\#\#}$P<0.01 *vs.* siC + dsDNA. RA, rheumatoid arthritis; FLSs, fibroblast like-synoviocytes; *FOXO1*, forkhead box 1; *pFOXO1*, phosphorylation of *FOXO1*; *MST1*, mammalian sterile 20-like kinase 1; *siMST1*, *MST1* siRNA; si*FOXO1*, *FOXO1* siRNA; siC, control siRNA; dsDNA, double-stranded DNA; qRT-PCR, quantitative reverse transcription-polymerase chain reaction.

or antimycin A (mitochondrial complex III inhibitor) abrogated ISD dsDNA-induced ROS production for 8 hours, while apocynin (NADPH oxidase inhibitor), AEBSF (NADPH oxidase inhibitor), carboxine (xanthine oxidase inhibitor), or oxypurinol (xanthine oxidase inhibitor) treatment did not affect ROS production, indicating that the mitochondrial ROS are the major source induced by ISD dsDNA (*Figure 6B*).

Next, we evaluated the effect of *cGAS* or *STING* inhibition on ROS production. Our results showed that *cGAS* or *STING* knockdown decreased the ROS levels induced by ISD dsDNA (*Figure 6C*), while treatment with rotenone or antimycin A did not influence the *cGAS* or *STING* expression (*Figure 6D*), implying that ROS induction occurs downstream of the *cGAS/STING* pathway. Finally, we investigated the role of ROS in regulating *MST1* and *FOXO1* activity. As shown in *Figure 6E*, treatment with rotenone or antimycin A diminished the phosphorylation of *MST1* and *FOXO1* in RA FLSs; however, *MST1* knockdown did not affect ISD dsDNA-induced ROS levels (*Figure 6F*). These data indicated that ROS operate upstream of the *MST1-FOXO1* pathway.

As a previous study reported an increased amount of mitochondrial ROS in RA FLSs (14), we aimed to further determine whether mitochondrial ROS affects the migration and invasion of RA FLSs. Our results showed that treatment with rotenone or antimycin A reduced the ISD dsDNA-induced migration and invasion of RA FLSs

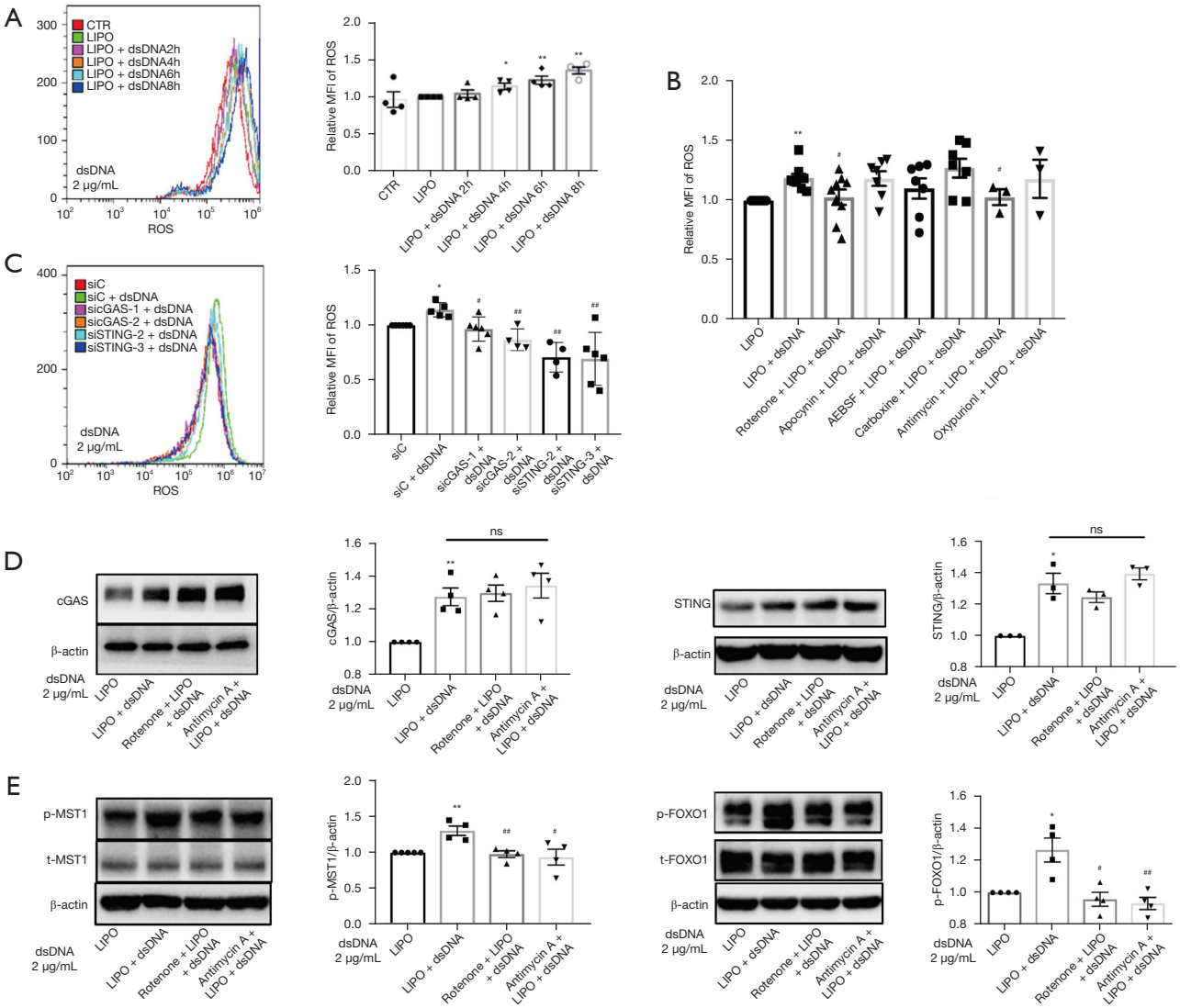

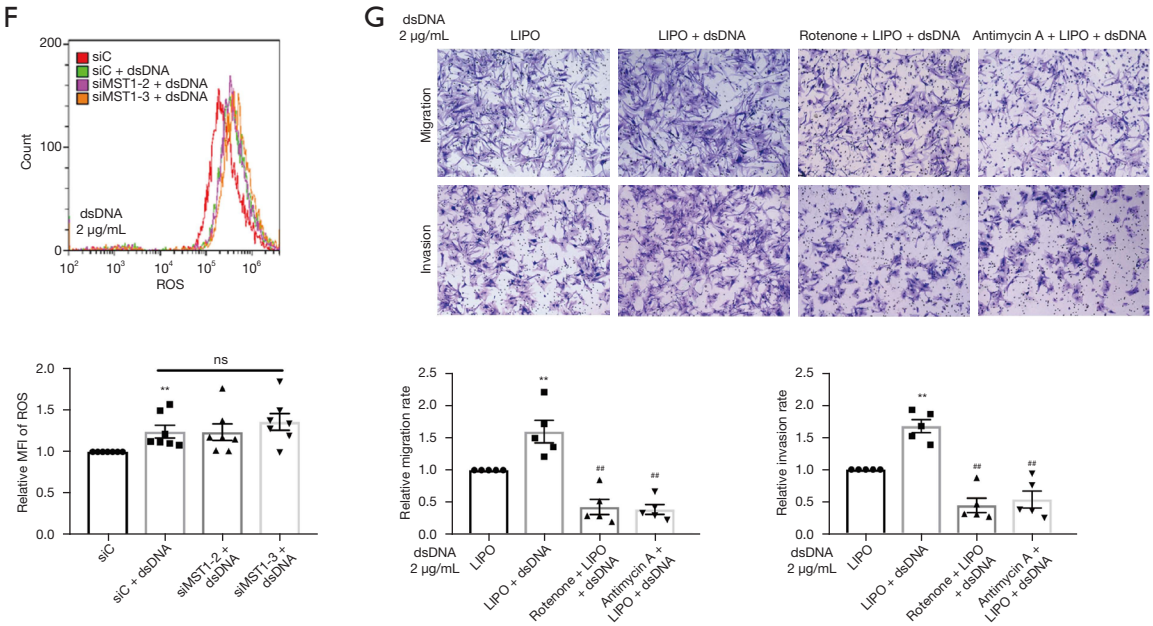

Figure 6 The effect of *cGAS/STING* inhibition on ROS production in RA FLSs. Protein expression was measured using western blotting. (A) The effect of ISD dsDNA on ROS production. RA FLSs were transfected with ISD dsDNA (2 μg/mL) at different times (2, 4, 6, and 8 hours). Representative plots of ROS level are shown. (B) RA FLSs were pretreated with rotenone (20 nM), apocynin (30 μM), AEBSF (2 μM), carboxin (5 μM), antimycin A (2 μg/mL), and oxypurinol (0.3 mM) for 24 hours and transfected with ISD dsDNA (2 μg/mL) for 8 hours. (C) The effect of *cGAS* or *STING* knockdown on ROS production. RA FLSs transfected with *cGAS*, *STING* siRNA, or control siRNA were serum-starved overnight and then transfected with dsDNA (2 μg/mL) for 8 hours. Graphs (A-C) show the relative MFI of ROS. (D,E) The effect of rotenone or antimycin A treatment on the expression of *cGAS* (D), *STING* (D), phosphorylated *MST1* (E), and phosphorylated *FOXO1* (E). RA FLSs were pretreated with rotenone (20 nM) or antimycin A (2 μg/mL) for 24 hours and then transfected with ISD dsDNA (2 μg/mL) for 24 hours (*cGAS* and *STING* group), 2 hours (*pMST1* group) or 8 hours (*pFOXO1* group). (F) The effect of *MST1* knockdown on ROS production. RA FLSs transfected with *MST1* siRNA or control siRNA were serum-starved overnight and transfected with dsDNA (2 μg/mL) for 8 hours. (G) The effect of ROS production on migration and invasion. RA FLSs were pretreated with rotenone (20 nM) or antimycin A (2 μg/mL) for 24 hours and then transfected with ISD dsDNA (2 μg/mL) for 8 hours. The relative migration and invasion rate was calculated by counting migrated or invaded cells and then through normalization to the lipo or lipo + dsDNA. Migrated and invaded cells on the membrane were stained with 0.3% crystal violet. Representative images (original magnification: 100×) are shown. Graphs show the relative migration rates. ns indicates no statistically significant difference. The data (A-G) are shown as the mean ± SEM from at least 3 independent experiments. *P<0.05; **P<0.01 *vs.* lipo; $^{\#}$P<0.05; $^{\#\#}$P<0.01 *vs.* lipo + dsDNA. RA, rheumatoid arthritis; FLSs, fibroblast like-synoviocytes; ROS, reactive oxygen species; LIPO, Lipofectamine 3000; CTR, control; *cGAS*, cyclic GMP-AMP synthase; *STING*, stimulator of interferon genes; *MST1*, mammalian sterile 20-like kinase 1; *FOXO1*, forkhead box 1; siC, control siRNA; *sicGAS*, *cGAS* siRNA; *siSTING*, *STING* siRNA; *siMST1*; *MST1* siRNA; dsDNA, double-stranded DNA; ns, no statistically significant difference; MFI, mean fluorescence intensity.

(*Figure 6G*). These findings suggested that mitochondrial ROS play an important role in regulating the migration and invasion of RA FLSs induced by ISD dsDNA.

Discussion

We found that transfection with synthetic dsDNA promotes the migration and invasion of RA FLSs, while *cGAS* or *STING* knockdown decreases dsDNA-induced migration and invasion. Furthermore, our results showed that *cGAS/STING* activation leads to increased mitochondrial ROS levels that promote *MST1* phosphorylation and subsequent phosphorylation and nuclear translocation of *FOXO1*. Furthermore, *cGAS/STING* activation may contribute to

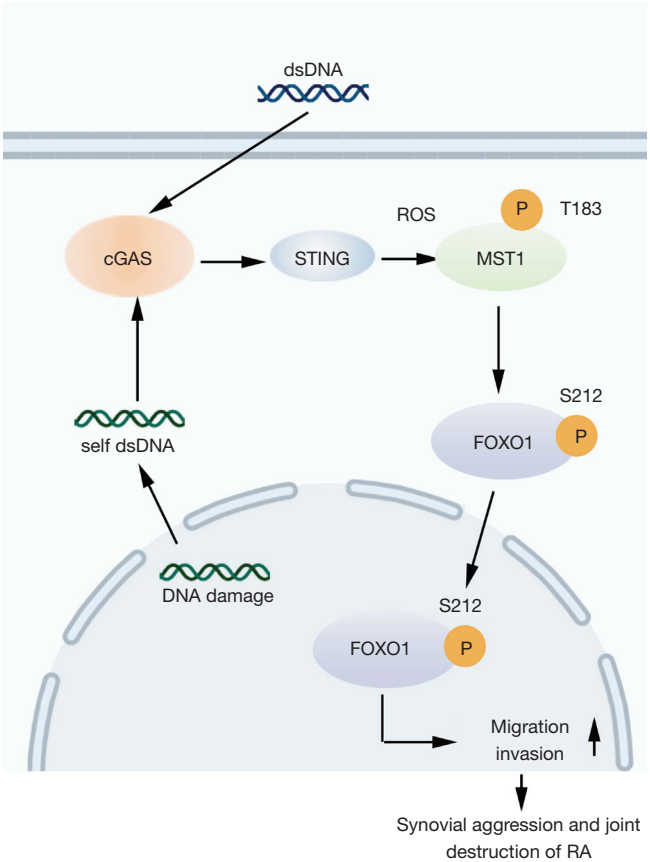

Figure 7 The proposed model for *cGAS/STING* activation mediated regulation of the migration and invasion of RA FLSs. RA, rheumatoid arthritis; FLSs, fibroblast like-synoviocytes; ROS, reactive oxygen species; *cGAS*, cyclic GMP-AMP synthase; *STING*, stimulator of interferon genes; *MST1*, mammalian sterile 20-like kinase 1; dsDNA, double-stranded DNA.

the aggressive behavior of RA FLSs by targeting *MST1*-mediated *FOXO1* (*Figure 7*).

Recent studies have indicated that the *cGAS/STING* pathway participates in regulating the migration of some cell lines and tumor metastasis. For instance, cytosolic mitochondrial DNA (mtDNA) can activate cytosolic DNA sensor *cGAS/STING* signaling to regulate endothelial cell migration and angiogenesis processes (8). Furthermore, *STING* knockdown was found to enhance cervical cancer cell migration (15), while *cGAS/STING* signal activation was shown to promote the maturation and migration of dendritic cells (16). In our study, we demonstrated that *cGAS* or *STING* inhibition also decreased the migration and invasion of cytosolic dsDNA-induced RA FLSs. Moreover, *cGAS* or *STING* knockdown blocked the invasion of RA FLSs into human cartilage implants transferred under the skin of SCID mice. A growing body of evidence indicates that the high invasive ability of FLSs is critical for joint destruction in RA; therefore, our findings suggest that the *cGAS/STING* pathway has an important role in controlling rheumatoid synovial aggression and joint destruction.

Hippo kinase *MST1* has emerged as a critical downstream target of the *cGAS/STING* pathway in the process of endothelial cell migration (8). To explore how the *cGAS/STING* pathway regulates RA FLSs functions, we evaluated the role of *cGAS/STING* in modulating *MST1* activation in RA FLSs. We determined that *cGAS* or *STING* knockdown suppressed dsDNA-induced *MST1* phosphorylation and that *MST1* inhibition reduced the migration and invasion of RA FLSs, suggesting that *MST1* mediates the role of *cGAS/STING* in controlling RA FLS migration. Consistent with our findings, it has been reported that *MST1* promotes the malignant proliferation and metastasis of tumor cells (17) and that *MST1* knockdown inhibits the proliferation and migration of T cells from psoriasis patients, indicating that *MST1* may be a target for the treatment of psoriasis (18). However, there are also reports that *MST1* overexpression inhibits the proliferation and migration of breast cancer cells (19), suggesting that *MST1* might possess a cell type-specific role in regulating cellular functions.

We further explored how *MST1* controls RA FLS functions. It is well known that the Hippo signaling pathway figures prominently in development, tissue homeostasis, and immune response. Dysregulation of Hippo signaling results in abnormal cell proliferation and neoplasia (20). In mammalian cells, Hippo signaling can be initiated by a series of upstream stimuli. In canonical signaling, activation of *MST1/2*, a core component of Hippo, results in subsequent phosphorylation of *LATS1/2*, and negatively modulates the Hippo pathway effector Yorkie (*YAP*/TAZ) (12). Therefore, we evaluated whether *MST1* regulates the phosphorylation of *LATS1* and *YAP*. We found that *MST1* knockdown did not affect the phosphorylation of *LATS1/2* or YAP in dsDNA-induced RA FLSs. This indicates that the *LATS1/YAP* pathway does not mediate the role of MST1 in regulating RA FLS functions. Similar to our results, netrin-1-induced YAP protein stability is not dependent on the Hippo kinase MST1/2 in various liver and glioblastoma cancer cells (21). Therefore, we speculated that *MST1* controls RA FLSs functions through alternative pathways.

Recent evidence shows that *MST1* regulates various cellular processes by activating the noncanonical Hippo pathways or alternative pathways and not the "canonical" Hippo pathway (22). Interestingly, recent studies show that *MST1* phosphorylates the transcription factor *FOXO1*, resulting in oxidative stress-induced neuronal cell death (23,24). The endothelial *MST1-FOXO1* cascade is critical for the directional migration of endothelial tip cells (24). Moreover, phosphorylation of *FOXO1* has been observed in RA FLSs (25). This prompted us to ascertain whether *FOXO1* mediates the role of *MST1* in RA FLS functions. As expected, we found that *MST1* knockdown decreased the dsDNA-induced phosphorylation of *FOXO1* and that *cGAS* or *STING* knockdown also inhibited the dsDNA-induced phosphorylation of *FOXO1*. Furthermore, *FOXO1* knockdown decreased the migration and invasion of RA FLSs. Collectively, these findings suggest that *MST1*-mediated *cGAS/STING* controls RA FLS migration and invasion via *FOXO1* and not via the "canonical" *LATS1-YAP* pathway.

It has been reported that ROS-mediated regulation of cell migration and tumor metastasis is dependent on the noncanonical Hippo *MST1/MST2*-FoxO3a-ΔNp63α pathway (26). ROS produced in the mitochondria can activate *MST1* in endothelial cells, promoting the nuclear import of *FOXO1* and augmenting its transcriptional regulation of polarity and migration-associated genes (27), which suggests that *MST1* is sensitive to oxidative stress. In our study, we found that *cGAS* or *STING* knockdown reduced ROS production and that a mitochondrial ROS inhibitor diminished the phosphorylation of *MST1* in ISD dsDNA-stimulated RA FLSs. Consistent with our findings, a previous study showed that oxidative stress stimulation increased *MST1* expression and promoted mitochondrial dysfunction in RA FLSs (13). We also observed that a mitochondrial ROS inhibitor reduced ISD dsDNA-induced migration and invasion of RA FLSs. Taken together, our findings suggest that the *cGAS/STING* activation may elicit mitochondrial ROS production, leading to *MST1* phosphorylation in RA FLSs.

In summary, we demonstrated that *cGAS/STING* signaling plays an important role in controlling rheumatoid synovial aggression via the mitochondrial ROS–mediated *MST1-FOXO1* pathway. This suggests that targeting *cGAS/STING* signaling might be a potential therapeutic strategy for RA.

Acknowledgments

The authors would like to thank Prof. Aishan He (Sun Yat-sen University, China) for providing a portion of the clinical samples.

Funding: This work was supported by grants from the National Natural Science Foundation of China (grants Nos. 81871275, 82071831, 81671591, 82001742, U1401222, and 81501389), the Guangzhou Science and Technology Project (Nos. 201803010042, and 202102020238), and the Guangdong Basic and Applied Basic Research Foundation (Nos. 2020A1515010221, 2021A1515010535).

Footnote

Reporting Checklist: The authors have completed the MDAR reporting checklist. Available at https://atm.amegroups.com/article/view/10.21037/atm-21-4533/rc

Data Sharing Statement: Available at https://atm.amegroups.com/article/view/10.21037/atm-21-4533/dss

Peer Review File: Available at https://atm.amegroups.com/article/view/10.21037/atm-21-4533/prf

Conflicts of Interest: All authors have completed the ICMJE uniform disclosure form (available at https://atm.amegroups.com/article/view/10.21037/atm-21-4533/coif). The authors have no conflicts of interest to declare.

Ethical Statement: The authors are accountable for all aspects of the work in ensuring that questions related to the accuracy or integrity of any part of the work are appropriately investigated and resolved. The study was conducted in accordance with the Declaration of Helsinki (as revised in 2013). This study was approved by the Medical Ethics Committee of the First Affiliated Hospital, Sun Yat-sen University, China (No. [2017]049), and informed consent was taken from all individual participants. All procedures involving animals were approved by the Institutional Animal Care and Use Committee (IACUC) of Sun Yat-sen University (No. SYSU-IACUC-2021-000028), according to the guidelines of the Chinese Ethics Committee for the care and use of animal research.

References

1. You S, Koh JH, Leng L, et al. The Tumor-Like Phenotype of Rheumatoid Synovium: Molecular Profiling and Prospects for Precision Medicine. Arthritis Rheumatol 2018;70:637-52.
2. Bottini N, Firestein GS. Duality of fibroblast-like synoviocytes in RA: passive responders and imprinted aggressors. Nat Rev Rheumatol 2013;9:24-33.
3. Svensson MND, Zoccheddu M, Yang S, et al. Synoviocyte-targeted therapy synergizes with TNF inhibition in arthritis reversal. Sci Adv 2020;6:eaba4353.
4. Yu L, Liu P. Cytosolic DNA sensing by cGAS: regulation, function, and human diseases. Signal Transduct Target Ther 2021;6:170.
5. Dong C, Liu Y, Sun C, et al. Identification of Specific Joint-Inflammatogenic Cell-Free DNA Molecules From Synovial Fluids of Patients With Rheumatoid Arthritis. Front Immunol 2020;11:662.
6. Wang J, Li R, Lin H, et al. Accumulation of cytosolic dsDNA contributes to fibroblast-like synoviocytes-mediated rheumatoid arthritis synovial inflammation. Int Immunopharmacol 2019;76:105791.
7. Guo Q, Chen X, Chen J, et al. STING promotes senescence, apoptosis, and extracellular matrix degradation in osteoarthritis via the NF-κB signaling pathway. Cell Death Dis 2021;12:13.
8. Yuan L, Mao Y, Luo W, et al. Palmitic acid dysregulates the Hippo-YAP pathway and inhibits angiogenesis by inducing mitochondrial damage and activating the cytosolic DNA sensor cGAS-STING-IRF3 signaling mechanism. J Biol Chem 2017;292:15002-15.
9. Ueda Y, Kondo N, Kinashi T. MST1/2 Balance Immune Activation and Tolerance by Orchestrating Adhesion, Transcription, and Organelle Dynamics in Lymphocytes. Front Immunol 2020;11:733.
10. Aletaha D, Neogi T, Silman AJ, et al. 2010 Rheumatoid arthritis classification criteria: an American College of Rheumatology/European League Against Rheumatism collaborative initiative. Arthritis Rheum 2010;62:2569-81.
11. Müller-Ladner U, Kriegsmann J, Franklin BN, et al. Synovial fibroblasts of patients with rheumatoid arthritis attach to and invade normal human cartilage when engrafted into SCID mice. Am J Pathol 1996;149:1607-15.
12. Taha Z, Janse van Rensburg HJ, Yang X. The Hippo Pathway: Immunity and Cancer. Cancers (Basel) 2018;10:94.
13. Wang Y, Yang Q, Shen S, et al. Mst1 promotes mitochondrial dysfunction and apoptosis in oxidative stress-induced rheumatoid arthritis synoviocytes. Aging (Albany NY) 2020;12:16211-23.
14. Fan XX, Xu MZ, Leung EL, et al. ROS-Responsive Berberine Polymeric Micelles Effectively Suppressed the Inflammation of Rheumatoid Arthritis by Targeting Mitochondria. Nanomicro Lett 2020;12:76.
15. Shi F, Su J, Wang J, et al. Activation of STING inhibits cervical cancer tumor growth through enhancing the anti-tumor immune response. Mol Cell Biochem 2021;476:1015-24.
16. Li A, Yi M, Qin S, et al. Activating cGAS-STING pathway for the optimal effect of cancer immunotherapy. J Hematol Oncol 2019;12:35.
17. Hong AW, Meng Z, Guan KL. The Hippo pathway in intestinal regeneration and disease. Nat Rev Gastroenterol Hepatol 2016;13:324-37.
18. Tang H, Guo Z, Tang X, et al. MST1 modulates Th17 activation in psoriasis via regulating TLR4-NF-κB pathway. Hum Cell 2021;34:28-36.
19. Jin X, Zhu L, Xiao S, et al. MST1 inhibits the progression of breast cancer by regulating the Hippo signaling pathway and may serve as a prognostic biomarker. Mol Med Rep 2021;23:383.
20. Meng Z, Moroishi T, Guan KL. Mechanisms of Hippo pathway regulation. Genes Dev 2016;30:1-17.
21. Qi Q, Li DY, Luo HR, et al. Netrin-1 exerts oncogenic activities through enhancing Yes-associated protein stability. Proc Natl Acad Sci U S A 2015;112:7255-60.
22. Chen L. Non-canonical Hippo signaling regulates immune responses. Adv Immunol 2019;144:87-119.
23. Lehtinen MK, Yuan Z, Boag PR, et al. A conserved MST-FOXO signaling pathway mediates oxidative-stress responses and extends life span. Cell 2006;125:987-1001.
24. Yuan Z, Lehtinen MK, Merlo P, et al. Regulation of neuronal cell death by MST1-FOXO1 signaling. J Biol Chem 2009;284:11285-92.
25. Ludikhuize J, de Launay D, Groot D, et al. Inhibition of forkhead box class O family member transcription

factors in rheumatoid synovial tissue. Arthritis Rheum 2007;56:2180-91.
26. Wang Y, Li J, Gao Y, et al. Hippo kinases regulate cell junctions to inhibit tumor metastasis in response to oxidative stress. Redox Biol 2019;26:101233.
27. Kim YH, Choi J, Yang MJ, et al. A MST1-FOXO1 cascade establishes endothelial tip cell polarity and facilitates sprouting angiogenesis. Nat Commun 2019;10:838.

(English Language Editors: C. Mullens and J. Gray)

Cite this article as: Li R, Lin W, Kuang Y, Wang J, Xu S, Shen C, Qiu Q, Shi M, Xiao Y, Liang L, Xu H. *cGAS/STING* signaling in the regulation of rheumatoid synovial aggression. Ann Transl Med 2022;10(8):431. doi: 10.21037/atm-21-4533